

Model Predictive Control of Z Source Inverter: Formulation & Simulation

Abtahi Reza¹, Rajesh Biswas²

Department of Electrical & Electronic Engineering, Chittagong University of Engineering & Technology, Chittagong, Bangladesh

¹abtahiee@gmail.com, ²rajeshctg56@gmail.com

Abstract—This paper presents Model Predictive Control (MPC) of impedance-source (commonly known as Z-source) inverter in a three phase network. The Z-source converter employs a unique impedance circuitry to couple the converter main circuit to the power source, thus employing unique features that cannot be obtained in the traditional voltage-source and current-source inverters where a capacitor and inductor are used respectively. A typical model for a three phase ZSI using balanced load is developed, where MPC due to its feedback control algorithm, predicted the future output current across the load and solved an optimization problem with a view to selecting the optimal control. The quality of output waveform has been analysed by maintaining the total harmonic distortion (THD) at an optimum level. Moreover, an inverse relationship between THD and Switching frequency is also noted. In addition, inductor current & capacitor voltage has also been tracked and effect on THD is analyzed by changing values in source side inductor & resistor.

Index Terms—Model Predictive Control, Z-Source Inverter

I. INTRODUCTION

Control techniques associated to power converters has been developed since the middle of 20th century. Since then it became a very active topic for research in the field of power electronics. Adapted with discrete time digital implementation, linear control, modulation scheme and nonlinear control based on hysteresis control are widely used in power electronics applications. On the contrary, more complex control strategies are implemented along with incorporation of digital signal processing technique, amongst them MPC is one of the most prominent ones. The main purpose of MPC is to precalculate the behavior of a specific model and thus to choose an optimal value of a control variable. Based on the implementation steps of MPC, firstly the reference (load voltage or current of power converters) is set by the designer; secondly the predicted variables are to be generated by a modulation stage; finally the predicted variables are used to be compared with reference variable, and the one closest to the reference will be chosen. MPC control therefore, allows multivariable system subjecting to constraints by formulating a control model of the object due to which MPC has been established as a widespread and systematic control approach. MPC control scheme has been applied for current control of converters, active filter, rectifiers, and uninterruptible power supplies.

The ZSI, on the other hand, advantageously utilizes the shoot through states to boost the dc bus voltage by gating on both the upper and lower switches of a phase leg unlike traditional VSI and CSI. Therefore, ZSI can buck or boost voltage to a desired output voltage that is greater than available dc bus voltage. So, ZSI provides low cost, reliable and highly efficient single stage structure for buck and boost

power conversion whereas, VSI and CSI operate in either boost mode (CSI) or buck mode (VSI), not in buck-boost mode. Also, the gate driver needs to be carefully designed so that electromagnetic interference resulting in misgating can be avoided, else may cause ST in a VSI or may cause an open inductor circuit in CSI, which can destroy the switches because of high current or voltage stresses. They are both vulnerable to EMI noise. While, ZSI overcomes all barriers of CSI and VSI as the equivalent switching frequency is six times greater than the switching frequency of the main inverter, which greatly reduces the required inductance of the Z-source network.

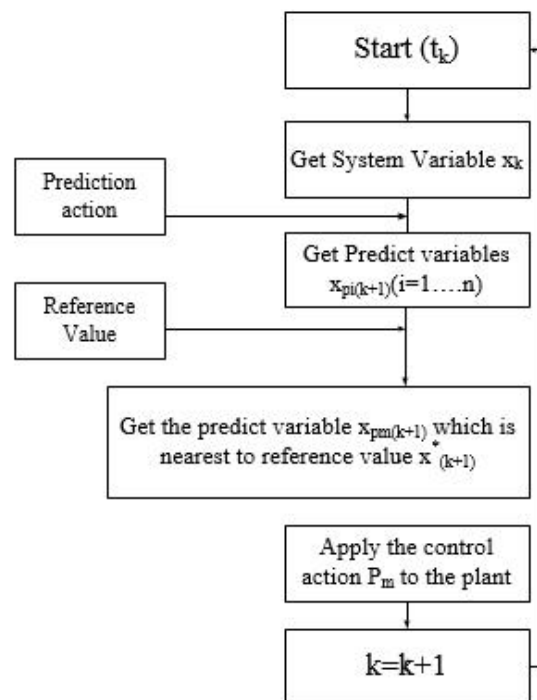


Fig. 1. Depiction of Model Predictive Control design using flowchart

Moreover, switches used in the converter can be a combination of switching devices and diodes, such as antiparallel, series and other combinations.

II. DESCRIPTION OF CONTROL STRATEGY

Although traditional modulation strategies such as pulse width modulation of Z- source inverter provides good output voltage waveform with specified modulation index and shoot-through ratio, there exists few feedback control methodology for Z-source inverter. Besides, with the presence of right half plane zero, non-minimal phase problem exists when transient response occurs due to which

complex modulation scheme has to be developed in order to make the transient process to be smooth. While, on the other hand, MPC provides quick reference tracking capability with simple feedback control method, and can help to reduce the non-phase minimal effect during transient process.

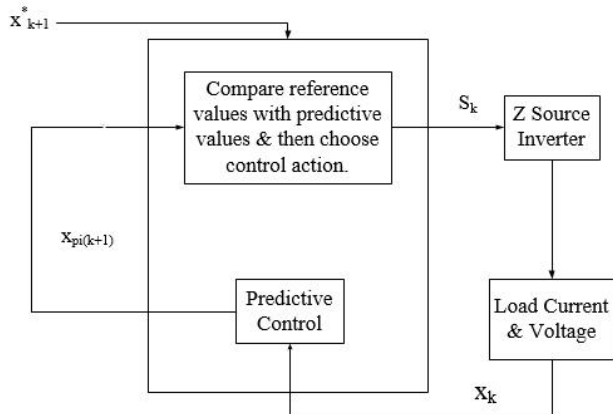


Fig. 2. Model Predictive Control of a typical Z Source Converter

Starting from time t_k , first step of MPC is to get current system variable x_k and reference variable x ; next get predictive variables $x_{p1(k+1)}, x_{p2(k+1)} \dots x_{pn(k+1)}$ by using predictive action $P_1, P_2 \dots P_n$; then compare these predictive variables with next sampling time reference value x_{k+1} , choose the one which is closest to the reference value; lastly, set $k = k + 1$ and repeat the process from the first step. The MPC control action is used as switching signals to control the 6 switches for a two-level three-phase Z-source inverter. Here, at first the system variable of Z-source inverter x_k , load current or voltage is measured. Then the predictive values is calculated by the predictive model. Next, by comparing the reference value with predictive values, the one which is closest to the reference value is chosen, and the corresponding control action will be used as switch signal to drive Z-source inverter. Then set $k = k + 1$ and repeat the steps.

III. INVERTER CONFIGURATION

A Z-source inverter is a type of power inverter, a circuit that converts direct current to alternating current. It functions as a buck-boost inverter without making use of DC-DC converter bridge due to its unique circuit topology. Impedance Z-Source networks provide an efficient means of power conversion between source and load in a wide range of electric power conversion applications. As capacitor and inductor is used in the d.c link, it acts as a constant high impedance voltage source. Z-source inverter basically operates in three modes. They are Normal Mode, Zero-state mode, Shoot-through mode.

In the first two mode that is normal & zero-state mode, ZSI operates as a traditional Pulse-width modulation (PWM) inverter. Due to the presence of last mode, Z-source greatly boost the dc source voltage with the help of conducting both switches of a phase leg. It should be noted that Z-source do not destroy the circuit while performing this operation due to its unique circuitry condition.

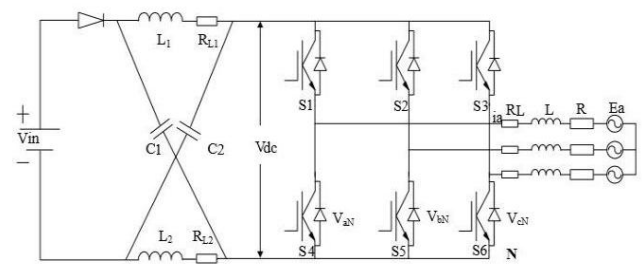


Fig. 3. Z-source inverter circuit configuration

TABLE I. SWITCHING STATES OF ZSI

State(output Voltage)	S1	S4	S2	S5	S3	S6
Active (finite) [100]	1	0	0	1	0	1
Active (finite) [110]	1	0	1	0	0	1
Active (finite) [010]	0	1	1	0	0	1
Active (finite) [011]	0	1	1	0	1	0
Active (finite) [001]	0	1	0	1	1	0
Active (finite) [101]	1	0	0	1	1	0
Null [000] (0V)	0	1	0	1	0	1
Null [111] (0V)	1	0	1	0	1	0
Shoot-Through E1(0V)	1	1	S2	!S2	S3	!S3
Shoot-Through E2(0V)	S1	!S1	1	1	S3	!S3
Shoot-Through E3(0V)	S1	!S1	S2	!S2	1	1
Shoot-Through E4(0V)	1	1	1	1	S3	!S3
Shoot-Through E5(0V)	1	1	S2	!S2	1	1
Shoot-Through E6(0V)	S1	!S1	1	1	1	1
Shoot-Through E7(0V)	1	1	1	1	1	1

In this above Table !S_x indicates complements of S_x where x = 1,2,3.

A. Switching circuit construction

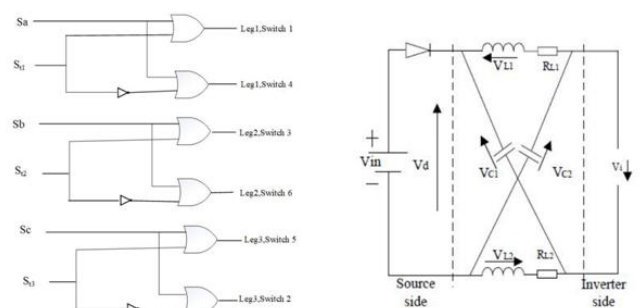


Fig. 4. Logic circuit to perform switching states

Switching States of ZSI indicates that ZSI performs total of 64 states $2^6 = 64$. To perform the switching states a logic circuit has constructed which is not similar to VSI. Each of the leg consists of one Shoot-through(St) signal. This signal paves the way of further output of this leg. If this Shoot-through signal sends binary 1, the output of the corresponding leg is such that both the switch conducts in the same leg which is not permissible in VSI. If this Shoot-through signal send binary 0, switching states will perform conventional VSI for the corresponding leg such as only one switch will conduct from each leg. So, a logic circuit has built in order to perform these 64 switching states.

B. Working Principle

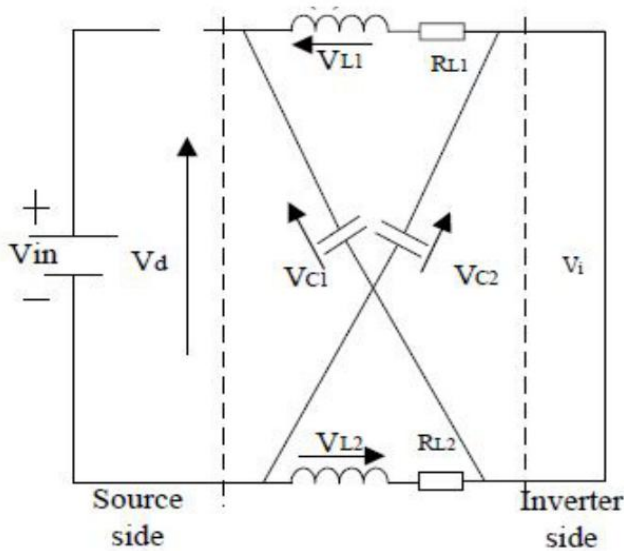


Fig. 5. Shoot-through states of ZSI

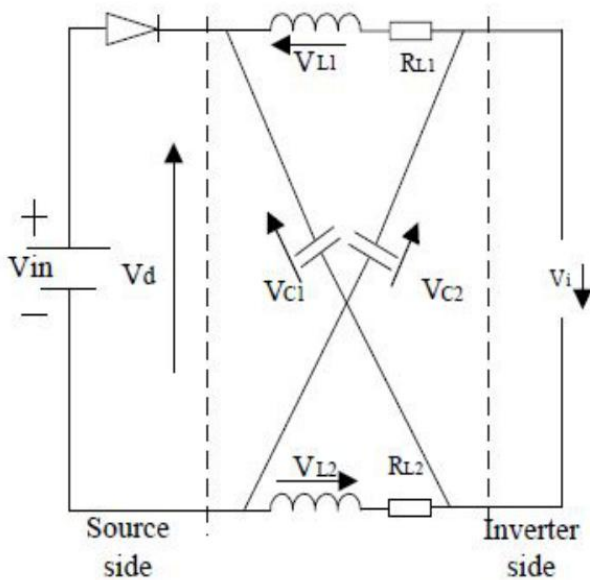


Fig. 6. Non Shoot-through states of ZSI

The above two figures represented two basic modes i.e. Normal mode and boost mode. The normal operation mode is not different from traditional inverter. The output voltage is solely depended on dc source voltage. However, in the later mode, Z-source increases the voltage at inverter bridge thus known as boost mode. The capacitor voltage plays the vital role to this network during Shoot-through states. In Fig.

5, it represents shoot through switching state. Z-source inverter simultaneously turned on two switches of one leg or two legs. During this state, diode D at input side turned off due to reverse bias. The capacitors play the role to charge the inductor and simultaneous operation can be performed.

Fig. 6 represents non shoot through states of ZSI. Diode D at input side conducts, The two capacitors do not involve in the operation as discharging occurs. During this state, only one switch in each leg is permissible to open like traditional VSI. The switching states of Z-source inverter can be determined by gating signals S_a, S_b and S_c as follows

$$S_a = \begin{cases} 1 & \text{if } S_1 \text{ on and } S_2 \text{ off} \\ 0 & \text{if } S_1 \text{ off and } S_2 \text{ on} \end{cases} \quad (1)$$

$$S_b = \begin{cases} 1 & \text{if } S_3 \text{ on and } S_4 \text{ off} \\ 0 & \text{if } S_3 \text{ off and } S_4 \text{ on} \end{cases} \quad (2)$$

$$S_c = \begin{cases} 1 & \text{if } S_5 \text{ on and } S_6 \text{ off} \\ 0 & \text{if } S_5 \text{ off and } S_6 \text{ on} \end{cases} \quad (3)$$

C. Output Load Current Prediction

The load current dynamics can be described by the vector differential equation

$$v = Ri + L \frac{di}{dt} + e \quad (4)$$

where v is the voltage vector generated by the inverter, i is the load current vector, and e the load back-emf vector. Note that for simulation and experimental results, the load back-emf is assumed to be sinusoidal with constant amplitude and constant frequency.

A discrete time form of load current with sampling time T_s can be used to predict the future value of the load current by utilizing the measured current at k th sampling instance. Finally, The required derivative $\frac{di_s}{dt}$ can be expressed as:

$$\frac{di_s}{dt} = \frac{i_s(k) - i_s(k-1)}{T_s} \quad (5)$$

By substituting the value, future load current is

$$i_s(k) = \frac{(v_s(k) - e_{load(k)})T_s + L_{load}i(k-1)}{R_{load}T_s + L_{load}} \quad (6)$$

The future load current can be determined by shifting the discret time equation:

$$i_s(k+1) = \frac{(v_s(k+1) - e_{load(k+1)})T_s + L_{load}i(k)}{R_{load}T_s + L_{load}} \quad (7)$$

D. Inductor current constraint

For a balanced network we can write,

$$R_{ind} = |i_{inds} - i_{inds(k+1)}| \quad (8)$$

Here, i_{inds} can be estimated as:

$$i_{inds} = \frac{P_{o/p}}{V_s}$$

Moreover $i_{inds(k+1)}$ can be expressed as two parts:

1) Nonshoot through state:

$$\dot{i}_{inds(k+1)} = \dot{i}_{L_s(k)} + \frac{T_s}{L_s}(V_s - V_{caps(k+1)} - R_{L_s}i_{inds(k)})$$

2) Shoot through state:

$$\dot{i}_{inds(k+1)} = \dot{i}_{L_s(k)} + \frac{T_s}{L_s}(V_{caps(k+1)} - R_{L_s}i_{inds(k)})$$

E. Capacitor voltage constraint

Similar to the inductor current constraint we will get:

$$R_{cap} = |V_{caps} - V_{caps(k+1)}| \quad (9)$$

Here V_{caps} is the next step capacitor voltage reference value which can be estimated as:

$$V_{caps} = 2 * V_{o/p}$$

$V_{caps(k+1)}$ is given as:

$$V_{caps(k+1)} = V_{caps(k)} + \frac{T_s}{C_s}(i_{ind(k+1)} - i_{inv(k+1)}) \quad (10)$$

F. Cost Function & Weighting factor

Minimization of the error between the measured currents and the reference values is the principal subject matter. This requirement can be written in the form of cost function which is expressed in orthogonal coordinates and measures the error between the references and the predicted controlled variables:

$$g = ||\mathbf{x}^*(k+1) - \mathbf{x}^P(k+1)||_2^2 \quad (11)$$

Where $\mathbf{x}^P(k+1)$ is predicted controlled vector and $\mathbf{x}^*(k+1)$ represents reference vector. In the model predictive control, as the future value of the reference is unknown, it is considered that the future value of the reference is approximately equal to the present value $\mathbf{x}^*(k+1) \approx \mathbf{x}^*(k)$.

Weighting factor put an importance to the control targets. With a higher weighting factor of a specific control target, the system will try to minimize the cost function for this particular control target. So, this factor should be designed carefully to achieve desired output from the system. But there is no procedure to measure the most favourable weighting factor while working with several control targets. Cost function incorporating weighting factor is:

$$g = \lambda_a |x^*(k+1) - x^P(k+1)| + \lambda_b |y^*(k+1) - y^P(k+1)| \quad (12)$$

where, λ depicts the weighing factor of the cost function. If $\lambda_a > \lambda_b$, system will give priority to minimize the error of x . On the other hand, if $\lambda_a < \lambda_b$, system will give priority to minimize the error of y

G. Cost Function Minimization

The formulated cost functions for load current, inductor current constraint & capacitor voltage constraint are given below:

$$C_{inv} = \|i_{ref} - i_{s(k+1)}\|_2^2 \quad (13)$$

$$R_{inds} = \|i_{inds} - i_{inds(k+1)}\|_2^2 \quad (14)$$

$$R_{caps} = \|V_{caps} - V_{caps(k+1)}\|_2^2 \quad (15)$$

Summing up all the constraints we get:

$$CF = w_1 C_{inv} + w_2 R_{inds} + w_3 R_{caps} \quad (16)$$

where w_1, w_2, w_3 are the weighting factors designed under different operating conditions.

H. Total Harmonic Distortion (THD) & Switching Frequency

Total Harmonic Distortion (THD) is defined as the ratio of the summation of all harmonic components to the fundamental frequency. It is a measurement of the presence of distortion in a signal. It is also known as distortion factor.

$$THD_F = \frac{\sqrt{V_2^2 + V_3^2 + V_4^2 + \dots}}{V_1} \quad (17)$$

where V_n is the RMS voltage of the nth harmonic and $n = 1$ is the fundamental frequency.

In power electronics, switching frequency (S.F.) refers to the rate at which a switching device turns ON and OFF. Switching frequency is evaluated by counting the number of on states in a time interval and by dividing this number by the inverters length. If we consider 12 active switches, then the average switching frequency per semiconductor will be:

$$f_{sw} = \lim_{N \rightarrow \infty} \frac{1}{NT_s} \sum_{\ell=0}^{N-1} \|u(\ell) - u(\ell-1)\|_1 \quad (18)$$

where $\|\cdot\|_1$ denotes the 1-norm and u denotes switching transition.

IV. SIMULATION RESULT

In this Z-source inverter model, few constant data set were selected by performing numerous possibilities. The best value has been selected and the model gives best output when it is performing under these conditions. These variables are given below & presented in a table :

From this model, output load current has been tracked. Analysis has been made for different weighting factor. The relationship between THD & Switching frequency has also been established.

TABLE II. MANIPULATED VARIABLES TO PERFORM SIMULATION

Variables	Representation	Values
v_{dc}	DC link Voltage	600(V)
R_{load}	Load resistant	10(Ω)
L_{load}	Load inductance	10(mH)
L_s	Source inductance	5(mH)
C_s	Source capacitor	1000(μ F)
f_{ref}	frequency reference	50(Hz)
T_s	Sample Time	20(μ s)

A. Current Control

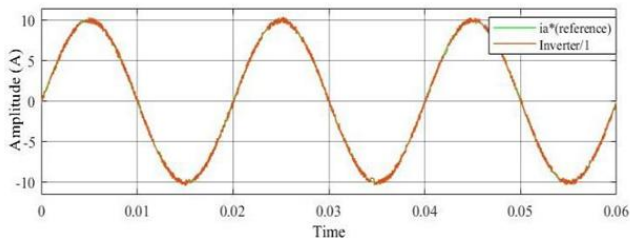


Fig. 7. Load current tracking

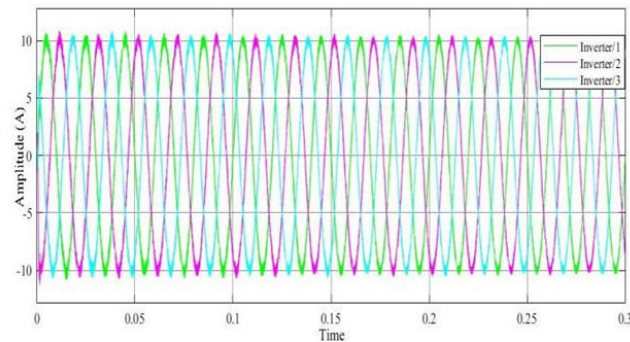


Fig. 8. Three phase load current

By taking the suitable data from Table 6.1, Load current has been tracked. The weighting factor is selected as 1 for load current. As from the figure below, it can be said that the current is not purely sinusoidal. Distortion is visible and THD is calculated from the figure. To observe the condition in all three legs, Three-phase load current has been evaluated in figure 8. The weighting factor is remain unchanged for the following observation.

B. Analysis of THD and Switching Frequency

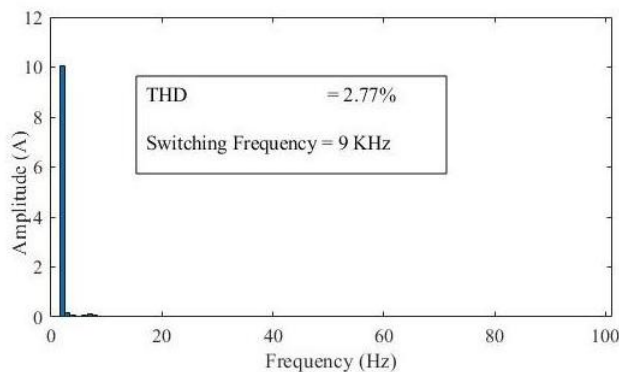


Fig. 9. % of THD & Switching frequency

From the above figures, it can be said that the current remain sinusoidal for most of the part. Little distortion can be seen from those figures. As the figures contain distortion, the total % of THD and switching frequency can be calculated from the above figures. Taking the weighting factor 1 for load current tracking the % of THD & Switching Frequency is evaluated. The first large bar represents fundamental component of load current which is 10A. From that above figure, The total % of THD is 2.77 and corresponding switching frequency for this THD is 9KHz. As the value of % of THD is less than 5% so this data represents appropriateness for practical applications. The THD can be varied widely by changing numerous parameters.

C. Effect of W.F. on THD & S.F.

At first, weighting factor 1 was selected and evaluated THD% Switching frequency for that value. Now a relationship between different weighting factor and THD has been established. The relationship between THD & Switching frequency has also been established. From the figure below, it can conclude that the lower the weighting factor the higher the % of THD. So, Z-source inverter model gives best output when weighting factor is selected high. The relationship between % of THD and switching frequency such that the higher the THD the lower the value of switching frequency. So to say, THD% switching frequency gives inverse relationship. Weighting Factor 0.1, 0.5 & 0.9 has been selected and the corresponding figure is given below :

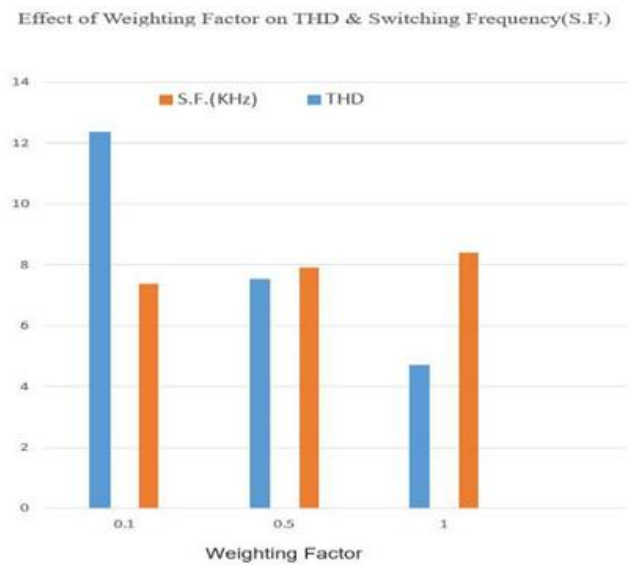


Fig. 10. THD & S.F. for different W.F.

D. Inductor Current Tracking

Taking $L = 5\text{mH}$, $C = 1000\mu\text{F}$ & weighting factor 0.85, inductor current has been tracked. This current bears significant amount of distortion due to internal property of inductor. There is also a solid reason for choosing the weighting factor 0.85. It gives lowest ripple for weighting factor 0.85. Inductor current contains high ripple so the effect of weighting factor in inductor current is appreciable. The figure is given below:

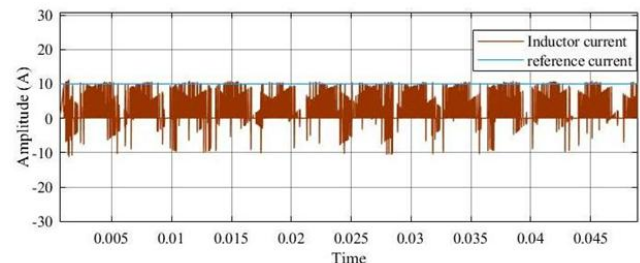


Fig. 11. Inductor Current Tracking

E. Capacitor Voltage Tracking

Finally, we evaluated the capacitor voltage in source side. During the Shoot-through state, capacitor voltage plays the main role to boost voltage. It actually helps to permit the shoot through state. This voltage is higher than the source

voltage. Capacitor voltage has been tracked & effect of selecting different weighting factor has also been presented in the figure below :

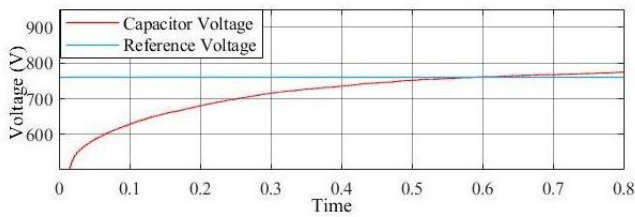


Fig. 12. Capacitor voltage tracking

As from the above figure, the capacitor voltage output is almost same as reference voltage after the transient part. The effect of weighting factor is very less for the distortion in this figure. By taking $L = 5\text{mH}$, $C = 1000\mu\text{F}$ & weighting factor 0.60, capacitor voltage has also been tracked. This voltage contains very less distortion & almost linear after the transient part of this model.

Effect of Inductor (L_s) & Resistor (R_s) in Source Side on THD Z-source inverter model contains inductor and resistor in source side. For different combination, % of THD varies differently. By testing different values for L_s and R_s , system gives best output when $L_s = 1\text{mH}$ and $R_s = 0.01$. This has been evaluated perfectly in the figure below. From this figure, for increasing the value of L_s & R_s , there is a significance change in THD. $L_s = 1\text{mH}$ and $R_s = 0.01$ it gives the best THD of 2.77%, as higher the value of L_s and R_s such that when $L_s = 50\text{mH}$ and $R_s = 0.05$, it crosses the THD value above 5% which is not suitable for a model. When $L_s = 90\text{mH}$ and $R_s = 1$, THD increases even higher and it crosses above 10%. By analyzing this figure, the best output happens when $L_s = 1\text{mH}$ and $R_s = 0.01$ so this value is taken for this model.

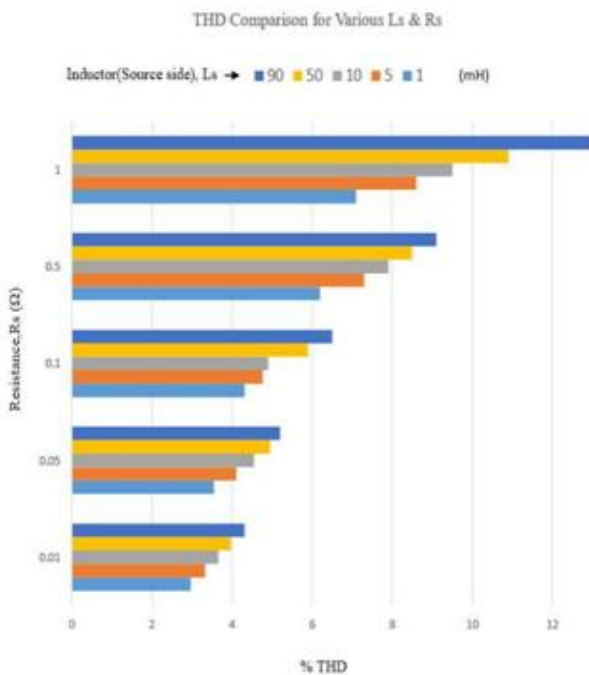


Fig. 13. Analysis of THD for different L_s & R_s

F. G. Effect of Inductor (L_s) & Resistor (R_s) in Source Side on Switching Frequency

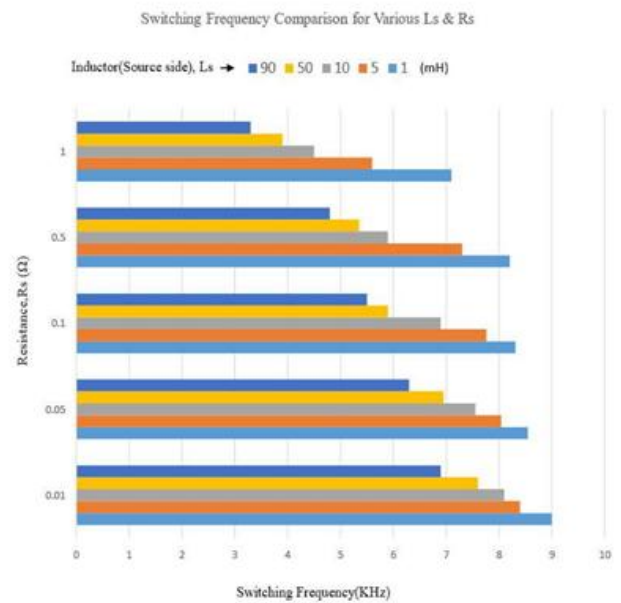


Fig. 14. Analysis of Switching frequency for different L_s & R_s

Switching frequency also varies for changing the value of L_s & R_s . The inverse relationship between THD and switching frequency has been established earlier. This has been widely evaluated in the figure given below. This figure represents switching frequency for different L_s & R_s . For $L_s = 1\text{mH}$ and $R_s = 0.01$ it gives the maximum switching frequency which is 9 KHz. THD is minimum for this switching frequency which has been represented in the previous figure. As the higher value for THD, this model gives lower switching frequency. As from the figure, for $L_s = 90\text{mH}$ and $R_s = 1$ the system model gives switching frequency of 3.3 KHz which is the minimum for this model and THD is maximum during this value.

V. CONCLUSION

Model predictive control of Z-source inverter has been evaluated in this paper. It consists of 64 states and the logic is different from conventional Voltage source inverter. However, it also represents how an inverter can work both on Shoot through and Non-Shoot through states by not damaging the model. This application is strictly prohibited in conventional VSI. Current control of Z-source inverter is analyzed and implemented.

After that, few regulations in source side has also been analyzed such as Inductor current and capacitor voltage. These are also tracked and the effect of changing these values has been plotted. These are nonlinear constraints and these can easily be included in this control method. Finally, absent of linear controller has confirmed that this MPC method doesn't require it. This ensures high speed tracking capability, reliable and stable on given circumstances. This thesis also evaluated Total harmonic distortion of load current and the corresponding switching frequency for that. The lower value of THD has also ensured the reliability of this model.

REFERENCES

- [1] J. Holtz, "pulsewidth modulation for power converters," Proc. IEEE, vol. 82, pp. 1194-1214, Aug 1994.
- [2] K. Thorborg, Power Electronics. London, U.K.: Prentice-Hall International (U.K.) Ltd., 1988.
- [3] M. H. Rashid, Power Electronics, 2nd ed. Englewood Cliffs, NJ: Prentice-Hall, 1993.
- [4] N. Mohan, W. P. Robbin, and T. Undeland, Power Electronics: Convert-ers, Applications, and Design, 2nd ed. New York: Wiley, 1995.
- [5] A. M. Trzynadlowski, Introduction to Modern Power Electronics. New York: Wiley, 1998.
- [6] B. K. Bose, Modern Power Electronics and AC Drives. Upper Saddle River, NJ: Prentice-Hall PTR, 2002.
- [7] P. T. Krein, Elements of Power Electronics. London, U.K.: Oxford Univ. Press, 1998.
- [8] O. Kukrer, "Discrete-time current control of voltagefed three-phase PWM inverters," IEEE Trans. Ind. Electron, vol. 11, pp. 260-269, Mar 1996.
- [9] R. Jos, P. Jorge, A. S. Csar, C. Pablo, L. Pablo, C. Patricio, and A. Ulrich, "Predictive Current Control of a Voltage Source Inverter," Industrial Electronics, IEEE Transactions on, vol. 54, pp. 495-503, 2007.
- [10] J. Seung-Gi and W. Myung-Ho, "DSP-based active power filter with predictive current control," Industrial Electronics, IEEE Transactions on, vol. 44, pp. 329-336, 1997.
- [11] L. Malesani, P. Mattavelli, and S. Buso, "Robust deadbeat current control for PWM rectifiers and active filters," Industry Applications, IEEE Transactions on, vol. 35, pp. 613-620, 1999.
- [12] S. Buso, S. Fasolo, and P. Mattavelli, "Uninterruptible power supply multiloop control employing digital predictive voltage and current regulators," Industry Applications, IEEE Transactions on, vol. 37, pp. 1846-1854, 2001.
- [13] P. Fang Zheng, "Z-source inverter," Industry Applications, IEEE Transactions on, vol. 39, pp. 504-510, 2003.
- [14] M. Fortunato, A. Giustiniani, and G. Petrone, et al., "Maximum power point tracking in a one-cycle-controlled single-stage photovoltaic in-verter," IEEE Trans. on Industrial Electronics, vol. 55, no. 7, pp. 2684-2693, 2008.
- [15] C. J. Gajanayake, D. M. Vilathgamuwa, and L. Poh Chiang, "Development of a Comprehensive Model and a Multiloop Controller for Z-Source Inverter DG Systems," Industrial Electronics, IEEE Transactions on, vol. 54, pp. 2352-2359, 2007.
- [16] L. Poh Chiang, D. M. Vilathgamuwa, C. J. Gajanayake, L. Yih Rong, and T. Chern Wern, "Transient Modeling and Analysis of Pulse-Width Modulated ZSource Inverter," Power Electronics, IEEE Transactions on, vol. 22, pp. 498-507, 2007.
- [17] W. Leonard, Control of Electric Drives. New York: Springer-Verlag, 1985.
- [18] R. E. Tarter, Principles of Solid-State Power Conversion. Indianapolis, IN: Sams, 1985.
- [19] R. D. Middlebrook and S. Cuk, Advances in Switched-Mode Power Conversion. Pasadena, CA: TESLaco, 1981, vol. I and II.
- [20] I. Takahashi and T. Noguchi, "A new quick response and high efficiency control strategy for an induction motor," IEEE Transactions on Industry Applications, vol. 22, no. 5, pp. 820-827, September 1986.
- [21] IEEE Standard Definitions for the Measurement of Electric Power Quantities Under Sinusoidal, Nonsinusoidal, Balanced, or Unbalanced Conditions, IEEE Std 1459-2010 (Revision of IEEE Std 1459-2000)
- [22] G.-A. Capolino, "Recent advances and applications of power electronics and motor drives-advanced and intelligent control techniques," in 34th Annual IEEE Conference on Industrial Electronics, IECON. pp. 37-39, November 2008.
- [23] P. Cortes, M. P. Kazmierkowski, R. M. Kennel, D. E. Quevedo, and J. Rodr'iguez, "Predictive control in power electronics and drives," IEEE Transactions on Industrial Electronics, vol. 55, no. 12, pp. 4312-4324, December 2008.
- [24] N. Femia, G. Petrone, and G. Spagnuolo, et al., "A technique for improving P& O MPPT performances of double-stage grid-connected photovoltaic systems," IEEE Trans. on Industrial Electronics, vol. 56, no. 11, pp. 4473-4482, 2009.
- [25] Abu-Rub H., Iqbal A., Moin Ahmed Sk., Peng F. Z., Li Y., Ge B., "Quasi-Z-source inverter-based photovoltaic generation system with maximum power tracking control using ANFIS," IEEE Transactions on Sustainable Energy, vol. 4, no. 1, pp. 11-20, Jan. 2013.
- [26] PREDICTIVE CONTROL OF POWER CONVERTERS AND ELEC-TRICAL DRIVES by Jose' Rodr'iguez and Patricio Cortes'. Universidad Tecnica Federico Santa Maria, Valparaiso, Chile.